Scattering of sound from point sources by multiple circular cylinders using addition theorem and superposition technique

Yi-Jhou Lin[1*], Ying-Te Lee[1] , I-Lin Chen[2] and Jeng-Tzong Chen[1,3]

[1]Department of Harbor and River Engineering
National Taiwan Ocean University, Keelung, Taiwan
[2]Department of Naval Architecture
National Kaohsiung Marine University, Kaohsiung, Taiwan
[3]Department of Mechanical and Mechatronics Engineering
National Taiwan Ocean University, Keelung, Taiwan
* E-mail: M96520007@mail.ntou.edu.tw

ABSTRACT

In this paper, we employ the addition theorem and superposition technique to solve the scattering problem with multiple circular cylinders arising from a point sound source. Using the superposition technique, the problem can be decomposed into two individual parts. One is the free-space fundamental solution. The other is a typical boundary value problem (BVP) with boundary conditions derived from the addition theorem by translating the fundamental solution. Following the success of null-field boundary integral formulation to solve the typical BVP of the Helmholtz equation with Fourier boundary densities, the second-part solution can be easily obtained after collocating the observation point exactly on the real boundary and matching the boundary condition. The total solution is obtained by superimposing the two parts which are the fundamental solution and the semi-analytical solution of the Helmholtz problem. An example was demonstrated to validate of the present approach. The parameters of size and spacing between cylinders are considered. The results are well compared with the available theoretical solutions and experimental data.
Keywords: addition theorem, superposition technique, null-field boundary integral formulation, Fourier series.

1. INTRODUCTION

Multiple scattering problems occur in many applications related to various areas of applied science, *e.g.* acoustics, electromagnetism, elasticity and water-wave problems. Mathematically speaking, the scattering field appears as the superposition of free field and radiation field. A better understanding of scattering phenomenon requires a precise knowledge of the influence of the different geometrical and physical parameters of the problem. Owing to the complexity of this problem, a numerical solution is always resorted, especially in the case where the number, radii and positions of objects are arbitrary. It can be consulted with the textbook of Martin [1].

Many researchers investigated the point-source problems in the past years. Row [2-3] successfully measured the experimental data of the interaction between two circular cylinders within an infinite domain. Sherer [4] developed an analytical method for solving the scattering problem with multiple rigid circular cylinders arranged in an arbitrary configuration. He used the Hankel transform method to calculate the incident field and determined the scattering fields from each cylinder in the collection through the separation of variables. Recently, Chen and his group developed the null-field integral equation in conjunction with the degenerate kernel to solve many engineering problems [5-8]. They claimed that their approach is a kind of semi-analytical approach since the error comes from truncating the terms of Fourier series. Five gains, mesh-free generation, well-posed model, principal value free, elimination of boundary-layer effect and exponential convergence are obtained. They also extended their approach to derive the anti-plane dynamic Green's function [9]. Not only perfect but also imperfect interface problems were addressed. Chen et al. [10] have proposed an indirect approach to construct the Green's function of Laplace operator by using the addition theorem and the superposition technique. In addition, Chou [11] utilized the addition theorem and superposition technique in the integral formulation to solve anti-plane problems with a circular boundary subject to a concentrated force and screw dislocation. He also proved the mathematical equivalence between the direct Green's-third-identity approach and superposition method for anti-plane elasticity problems subject to a concentrated force.

In this paper, the addition theorem and superposition technique are employed to solve the scattering problem with multiple circular cylinders arising from point sound sources. The problem is decomposed into two parts. One

is the problem of the fundamental solution for the free field. The other is a typical BVP with boundary conditions derived from the addition theorem by translating the fundamental solution. Following the success of null-field boundary integral formulation in conjunction with degenerate kernel to solve the typical BVP, the second part solution can be easily obtained after collocating the observation point exactly on the real boundary and matching boundary condition. The total solution is obtained by superimposing the two parts. An example was demonstrated to validate the proposed approach. The parameters of size and spacing of cylinders are considered. The results are compared well with the available theoretical solutions and experimental data.

2. NULL-FIELD BOUNDARY INTEGRAL EQUATION METHOD FOR A TYPICAL BVP

2.1 Problem statements

A typical BVP with H randomly distributed circular cylinders bounded in an infinite domain enclosed with the boundaries, B_j ($j = 1, 2, \cdots, H$),

$$B = \bigcup_{j=1}^{H} B_j. \qquad (1)$$

is considered here. The field variable $u(x)$ satisfy

$$(\nabla^2 + k^2)u(x) = 0, \quad x \in D, \qquad (2)$$

where D is the domain, ∇^2 is the Laplacian operator, k is the wave number which is the angular frequency over the speed of sound. The boundary condition can be specified to either Dirichlet or Neumann type as follows:

$$u(x) = \bar{u}, \quad x \in B, \qquad (3)$$

$$\text{or } \frac{\partial u(x)}{\partial n_x} = \bar{t}, \quad x \in B. \qquad (4)$$

This problem is a typical BVP, and can be easily solved by using the null-field boundary integral equation approach.

2.1 Dual null-field integral formulation — the conventional version

Based on the dual boundary integral formulation [5] for the domain point, we have

$$2\pi u(x) = \int_B T(s,x)u(s)dB(s)$$
$$- \int_B U(s,x)\frac{\partial u(s)}{\partial n_s}dB(s), \quad x \in D, \qquad (5)$$

$$2\pi \frac{\partial u(x)}{\partial n_x} = \int_B M(s,x)u(s)dB(s)$$
$$- \int_B L(s,x)\frac{\partial u(s)}{\partial n_s}dB(s), \quad x \in D, \qquad (6)$$

where s and x are the source and field points, respectively. B is the boundary, n_x and n_s denote the outward normal vector at field point and source point, respectively. and the kernel function $U(s,x)$ is the fundamental solution which satisfies

Fig. 1 An infinite plane with arbitrary number of circular cylinders subject to the Dirichlet or Neumann boundary conditions.

$$(\nabla^2 + k^2)U(s,x) = \delta(x - s), \qquad (7)$$

where $\delta(x - s)$ denotes the Dirac-delta function. The other kernel functions can be obtained as

$$T(s,x) = \frac{\partial U(s,x)}{\partial n_s}, \qquad (8)$$

$$L(s,x) = \frac{\partial U(s,x)}{\partial n_x}, \qquad (9)$$

$$M(s,x) = \frac{\partial^2 U(s,x)}{\partial n_s \partial n_x}. \qquad (10)$$

By moving the field point x to the boundary, the dual boundary integral equations for the boundary point can be obtained as follows:

$$\pi u(x) = C.P.V. \int_B T(s,x)u(s)dB(s)$$
$$- R.P.V. \int_B U(s,x)\frac{\partial u(s)}{\partial n_s}dB(s), \quad x \in B, \qquad (11)$$

$$\pi \frac{\partial u(x)}{\partial n_x} = H.P.V. \int_B M(s,x)u(s)dB(s)$$
$$- C.P.V. \int_B L(s,x)\frac{\partial u(s)}{\partial n_s}dB(s), \quad x \in B, \qquad (12)$$

where $R.P.V.$ is the Riemann principal value, $C.P.V.$ is the Cauchy principal value and $H.P.V.$ is the Hadamard (or called Mangler) principal value. By moving the field point to the complementary domain, the dual null-field integral equations are shown as:

$$0 = \int_B T(s,x)u(s)dB(s)$$
$$- \int_B U(s,x)\frac{\partial u(s)}{\partial n_s}dB(s), \quad x \in D^c, \qquad (13)$$

$$0 = \int_B M(s,x)u(s)dB(s)$$
$$- \int_B L(s,x)\frac{\partial u(s)}{\partial n_s}dB(s), \quad x \in D^c, \qquad (14)$$

where the "D^c" denotes the complementary domain.

2.2 Dual null-field integral formulation — the present version

By introducing the degenerate kernels, the collocation point can be located on the real boundary

without facing singularity. Therefore, the representations of integral equations including the boundary point can be written as

$$2\pi u(x) = \int_B T(s,x)u(s)dB(s)$$
$$- \int_B U(s,x)\frac{\partial u(s)}{\partial n_s}dB(s), \quad x \in D \cup B, \quad (15)$$

$$2\pi \frac{\partial u(x)}{\partial n_x} = \int_B M(s,x)u(s)dB(s)$$
$$- \int_B L(s,x)\frac{\partial u(s)}{\partial n_s}dB(s), \quad x \in D \cup B, \quad (16)$$

and

$$0 = \int_B T(s,x)u(s)dB(s)$$
$$- \int_B U(s,x)\frac{\partial u(s)}{\partial n_s}dB(s), \quad x \in D^c \cup B, \quad (17)$$

$$0 = \int_B M(s,x)u(s)dB(s)$$
$$- \int_B L(s,x)\frac{\partial u(s)}{\partial n_s}dB(s), \quad x \in D^c \cup B, \quad (18)$$

once the kernel is expressed in terms of an appropriate degenerate form. It is found that the collocation point is categorized to three regions, domain (Eqs.(5)-(6)), boundary (Eqs.(11)-(12)) and complementary domain (Eqs.(13)-(14)) in the conventional formulation. After using the degenerate kernel for the null-field BIEM, Eqs.(15)-(16) and Eqs.(17)-(18) can include the boundary point.

2.3 Expansions of the fundamental solution and boundary density

The closed-form fundamental solution as previously mentioned is

$$U(s,x) = \frac{-iH_0^{(1)}(kr)}{4} \quad (19)$$

where $r \equiv |s - x|$ is the distance between the source point and the field point, $H_0^{(1)}$ is the first kind Hankel function of zeroth order, and i is the imaginary number of $i^2 = -1$. To fully utilize the property of circular geometry, the mathematical tools, degenerate (separable or of finite rank) kernel and Fourier series, are adopted for the analytical calculation of boundary integrals.
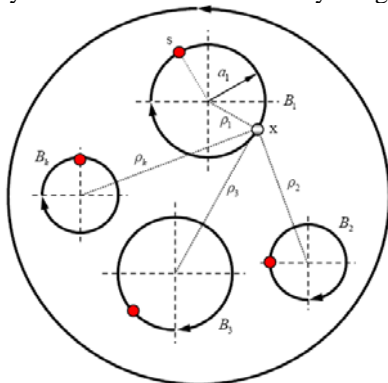
Fig. 2 Sketch of the null-field integral equation in conjunction with the adaptive observer system.

2.3.1 Degenerate (separable) kernel for fundamental solutions

In the polar coordinate, the field point x and source point s can be expressed an (ρ, ϕ) and (R, θ), respectively. By employing the addition theorem for separating the source point and field point, the kernel functions, $U(s,x)$, $T(s,x)$, $L(s,x)$ and $M(s,x)$, are expanded in terms of degenerate kernel as shown below:

$$U(s,x) = \begin{cases} U^i(s,x) = \dfrac{-i}{4}\sum\limits_{m=0}^{\infty}\varepsilon_m J_m(k\rho)H_m^{(1)}(kR) \\ \qquad\qquad \cos[m(\theta-\phi)], \quad R \geq \rho, \\ U^e(s,x) = \dfrac{-i}{4}\sum\limits_{m=0}^{\infty}\varepsilon_m J_m(kR)H_m^{(1)}(k\rho) \\ \qquad\qquad \cos[m(\theta-\phi)], \quad R < \rho, \end{cases} \quad (20)$$

$$T(s,x) = \begin{cases} T^i(s,x) = \dfrac{-ki}{4}\sum\limits_{m=0}^{\infty}\varepsilon_m J_m(k\rho)H_m'^{(1)}(kR) \\ \qquad\qquad \cos[m(\theta-\phi)], \quad R > \rho, \\ T^e(s,x) = \dfrac{-ki}{4}\sum\limits_{m=0}^{\infty}\varepsilon_m J_m'(kR)H_m^{(1)}(k\rho) \\ \qquad\qquad \cos[m(\theta-\phi)], \quad R < \rho, \end{cases} \quad (21)$$

$$L(s,x) = \begin{cases} L^i(s,x) = \dfrac{-ki}{4}\sum\limits_{m=0}^{\infty}\varepsilon_m J_m'(k\rho)H_m^{(1)}(kR) \\ \qquad\qquad \cos[m(\theta-\phi)], \quad R > \rho, \\ L^e(s,x) = \dfrac{-ki}{4}\sum\limits_{m=0}^{\infty}\varepsilon_m J_m(kR)H_m'^{(1)}(k\rho) \\ \qquad\qquad \cos[m(\theta-\phi)], \quad R < \rho, \end{cases} \quad (22)$$

$$M(s,x) = \begin{cases} M^i(s,x) = \dfrac{-k^2 i}{4}\sum\limits_{m=0}^{\infty}\varepsilon_m J_m'(k\rho)H_m'^{(1)}(kR) \\ \qquad\qquad \cos[m(\theta-\phi)], \quad R \geq \rho, \\ M^e(s,x) = \dfrac{-k^2 i}{4}\sum\limits_{m=0}^{\infty}\varepsilon_m J_m'(kR)H_m'^{(1)}(k\rho) \\ \qquad\qquad \cos[m(\theta-\phi)], \quad R < \rho, \end{cases} \quad (23)$$

where the superscripts "i" and "e" denote the interior and exterior cases for the expressions of kernel, respectively, and ε_m is the Neumann factor

$$\varepsilon_m = \begin{cases} 1, & m = 0, \\ 2, & m = 1, 2, \cdots, \infty. \end{cases} \quad (24)$$

It is noted that U and M kernels in Eqs.(20) and (23) contain the equal sign of $\rho = R$ while T and L kernels do not include the equal sign due to discontinuity.

2.3.2 Fourier series expansion for boundary densities

We apply the Fourier series expansion to approximate the boundary density and its normal derivative as expressed by

$$u(s) = a_0 + \sum_{n=1}^{\infty}(a_n \cos n\theta + b_n \sin n\theta), \quad s \in B, \quad (25)$$

$$\frac{\partial u(s)}{\partial n_s} = p_0 + \sum_{n=1}^{\infty}(p_n \cos n\theta + q_n \sin n\theta), \quad s \in B, \quad (26)$$

where a_n, b_n, p_n and q_n (n=0,1,2,…) are the Fourier coefficients and θ is the polar angle. In the real computation, the integrals can be analytically calculated

by employing the orthogonal property of Fourier series and only M terms is used in the summation instead of infinite terms. The present method is one kind of semi-analytical methods since errors only occur from the truncation of Fourier series.

2.4 Adaptive observer system

In order to fully employ the property of degenerate kernels for circular boundaries, an adaptive observer system is addressed as shown in Fig. 2. For the boundary integrals, the origin of the observer system can be adaptively located on the center of the corresponding boundary contour. The dummy variable in the circular boundary integration is the angle θ instead of radial coordinate R. By using the adaptive system, all the integrals can be easily calculated for multiply-connected problems.

2.5 Linear algebraic equation

In order to calculate the Fourier coefficients, N ($N=2M+1$) boundary nodes for each circular boundary are located uniformly on each circular boundary. From Eqs.(17) and (18), we have

$$0 = \sum_{i=1}^{H} \int_{B_i} T(s,x)u(s)dB(s)$$
$$- \sum_{i=1}^{H} \int_{B_i} U(s,x)\frac{\partial u(s)}{\partial n_s}dB(s), x \in D^c \cup B, \quad (27)$$

$$0 = \sum_{i=1}^{H} \int_{B_i} M(s,x)u(s)dB(s)$$
$$- \sum_{i=1}^{H} \int_{B_i} L(s,x)\frac{\partial u(s)}{\partial n_s}dB(s), x \in D^c \cup B. \quad (28)$$

It is noted that the integration path is clockwise. For the integral of the circular boundary B_i, the kernels ($U(s,x)$, $T(s,x)$, $L(s,x)$ and $M(s,x)$) are expressed by using the degenerate kernel and setting the origin at the center of B_i. The boundary densities ($u(s)$ and $\frac{\partial u(s)}{\partial n_s}$) are substituted by using the Fourier series. After discretizing Eq.(27), a linear algebraic system yields

$$[U]\{t\} = [T]\{u\}, \quad (29)$$

where $[U]$ and $[T]$ are the influence matrices with a dimension of $H \times (2M+1)$ by $H \times (2M+1)$, $\{u\}$ and $\{t\}$ denote the column vectors of Fourier coefficients with a dimension of $H \times (2M+1)$ by 1 for u and $\frac{\partial u}{\partial n}$, respectively. All the unknown coefficients can be solved by using the linear algebraic equation. Then the unknown boundary data can be determined and the potential is obtained by substituting the boundary data into Eq.(15). Based on the null-field integral equation approach, successful applications to Laplace, Helmholtz, biharmonic and biHelmholtz problems were presented in [5-8, 12-25].

3. METHODS OF SOLUTION

3.1 Problem statements
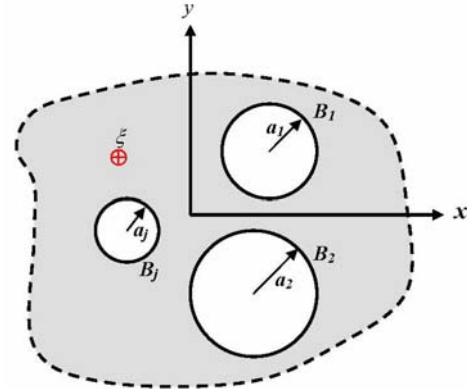
Fig.3 Infinite plane with arbitrary number of circular cylinders subject to a point sound source at ξ.
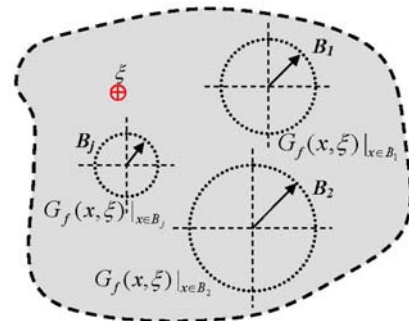
Fig. 4(a) Free field of the fundamental solution.
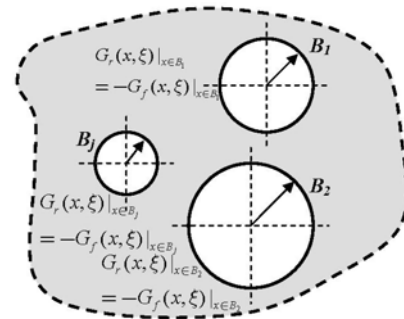
Fig. 4(b) Radiation field (a typical BVP).

The problem which we would like to solve is the scattering problem with multiple cylinders arising from a point source as shown in Fig.3. The problem is governed by the Helmholtz operator as follows:

$$(\nabla^2 + k^2)G(x,\xi) = \delta(x-\xi), \quad x \in D, \quad (30)$$

and the boundary is bounded by

$$B = \bigcup_{j=1}^{H} B_j. \quad (31)$$

Here, the cylinder is specified to be the soft boundary as

$$G(x,\xi) = 0, \quad x \in B, \quad (32)$$

The proposed approach for solving the problem will be elaborated on in the next section.

3.2 Green's function using the addition theorem and superposition technique

The scattering problem subject to a point sound source is shown in Fig.3. It can be decomposed into two parts: fundamental solution (free field) and radiation field, as shown in Figs.4(a) and 4(b). Based on the addition
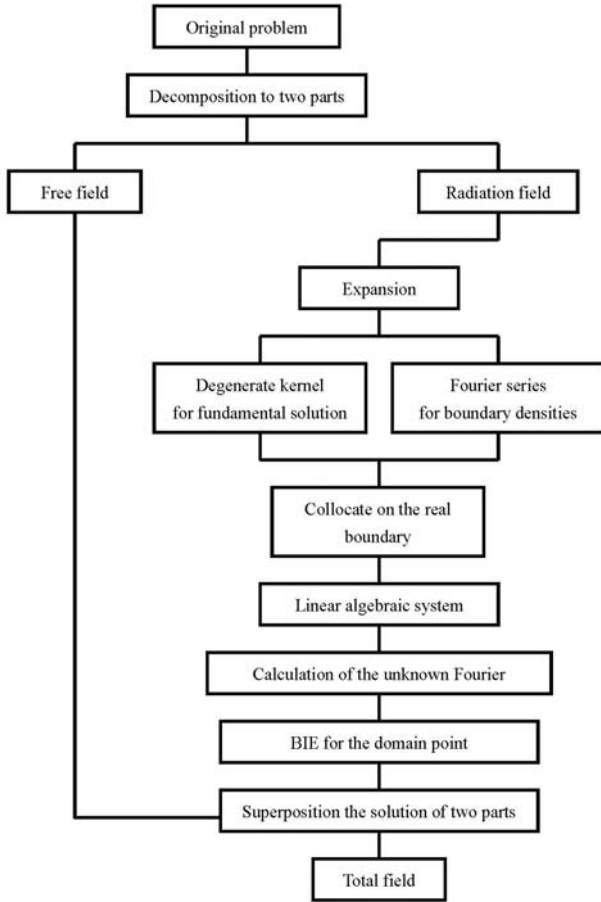

Fig.5 Flowchart of the present approach.

theorem, the fundamental solution can be separated into the series form using Eq.(20). For matching the boundary condition, the superposition of the artificial boundary condition ($G_f(x,\xi)$) in Fig.4(a) and the radiation boundary condition ($G_r(x,\xi)$) in Fig.4(b) must satisfy the original boundary condition in Fig.3. The second part (radiation field) is a typical BVP and can be easily solved by employing the null-field integral equation approach as mentioned in Section 2. For clarity, the flowchart of our method is shown in Fig.5.

3.3 Green's third-identity approach

Based on the Green's third identity, two systems, u and v, yield

$$\int_D u(x)\nabla^2 v(x)dD(x) = \int_B u(x)\frac{\partial v(x)}{\partial n}dB(x) \\ - \int_D \nabla u(x)\nabla v(x)dD(x), \tag{33}$$

$$\int_D [u(x)\nabla^2 v(x)dD(x) - v(x)\nabla^2 u(x)dD(x)] \\ = \int_B [u(x)\frac{\partial v(x)}{\partial n} - v(x)\frac{\partial u(x)}{\partial n}]dB(x). \tag{34}$$

By selecting u as the fundamental solution $U(x,s)$ and v as the Green's function $G(s,\xi)$, the Green's third identity gives:

$$2\pi G(x,\xi) = \int_B T(s,x)G(s,\xi)dB(s) \\ - \int_B U(s,x)\frac{\partial G(s,\xi)}{\partial n_s}dB(s) \tag{35} \\ + U(\xi,x), \quad x \in D.$$

3.4 Equivalence between the solution using the Green's third identity and superposition technique

The boundary integral equation for the free field problem can be written as:

$$2\pi G_f(x,\xi) = \int_B T(s,x)G_f(s,\xi)dB(s) \\ - \int_B U(s,x)\frac{\partial G_f(s,\xi)}{\partial n_s}dB(s) \tag{36} \\ + U(\xi,x), \quad x \in D,$$

where $G_f(x,\xi)$ is the free field. The boundary integral equation for the typical boundary value problem can be written as

$$2\pi G_r(x,\xi) = \int_B T(s,x)G_r(s,\xi)dB(s) \\ - \int_B U(s,x)\frac{\partial G_r(s,\xi)}{\partial n_s}dB(s), x \in D. \tag{37}$$

where $G_r(x,\xi)$ is the second part solution for the typical BVP. By superimposing G_f and G_r in Eqs.(36) and (37), respectively, we have

$$2\pi[G_f(s,\xi) + G_r(s,\xi)] \\ = \int_B T(s,x)[G_f(s,\xi) + G_r(s,\xi)]dB(s) \\ - \int_B U(s,x)\left[\frac{\partial G_f(s,\xi)}{\partial n_s} + \frac{\partial G_r(s,\xi)}{\partial n_s}\right]dB(s) \tag{38} \\ + U(\xi,x), \quad x \in D.$$

where $G_f(s,\xi) + G_r(s,\xi)$ and $\frac{\partial G_f(s,\xi)}{\partial n_s} + \frac{\partial G_r(s,\xi)}{\partial n_s}$

must satisfy the original boundary conditions. By comparing Eq.(38) with Eq.(35), we can find $G(x,\xi) = G_f(x,\xi) + G_r(x,\xi)$. Therefore, we have proven the mathematical equivalence between the solution of Green's third identity and that of superposition technique.

4. AN ILLUSTRACTIVE EXAMPLE

We consider an infinite plane with two identical circular cylinders subject to a point sound source as shown in Fig. 6. The radii of the two identical cylinders are a. The locations of source and probe are at $(-100,0)$ and $(2\lambda,y)$, respectively , where λ is the wave length. The distance between the two centers of identical cylinders is $2b$. The boundary conditions are the Dirichlet types ($G(x,\xi) = 0$) due to the soft cylinder. The potential distribution along the artificial boundary for the
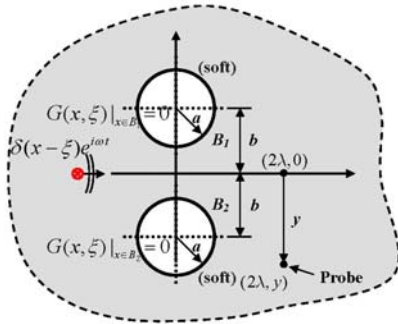
Fig. 6 An infinite plane with two equal circular cylinders subject to a point sound source.

free field is shown in Figs. 7 and 8 versus circular boundary and polar angle, respectively. Both the closed-form formula of Eq.(19) and series-form formula of Eq.(20) are given. After obtaining the total field at the probe, the relative amplitude is defined by dividing the total field with respect to the free field at ($2\lambda,0$). By considering $\lambda = \pi$, $b = \frac{1}{2}\pi$ and $a = 0.05\lambda$, the relative amplitude of the total field versus y of probe location is shown in Fig.9. The result agrees well with theoretical results and experimental data by Row [2].
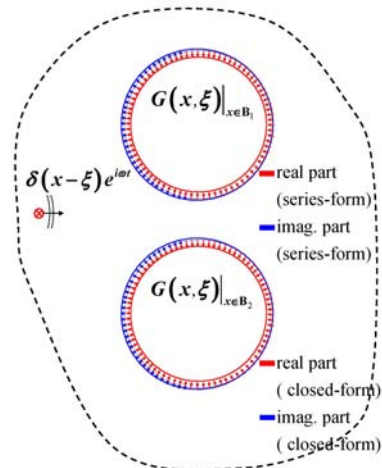
Fig. 7 Distribution potential on the artificial boundaries in the free field (upper part: series-form, lower part: closed-form, *M*=20).
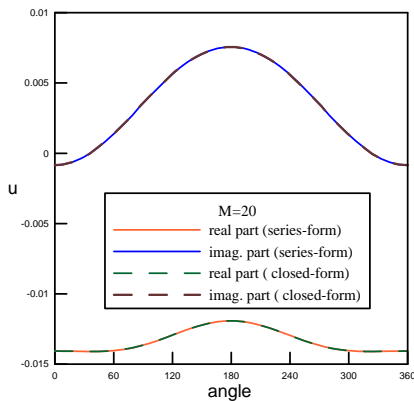
Fig. 8 Distribution potential on the artificial boundaries in the free field versus polar angle.
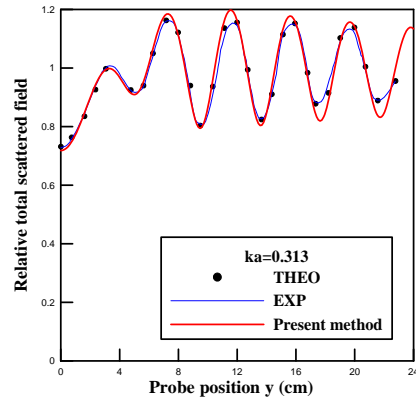
Fig. 9 Relative amplitude of total field versus the probe location y (*M*=20).
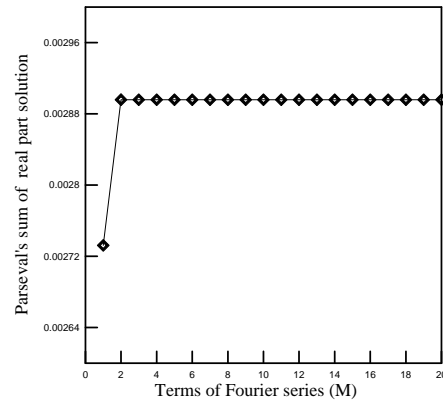
Fig. 10(a) Convergence test of Parseval's sum for $\partial G(x,\xi)/\partial n_x$ (real part).
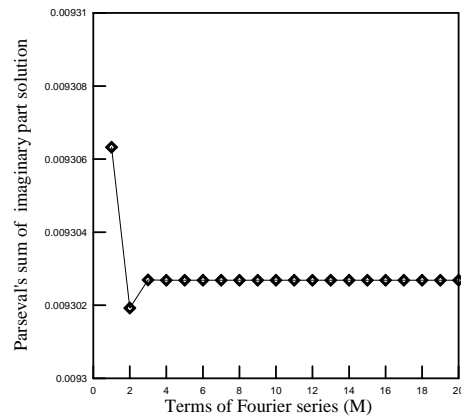
Fig. 10(b) Convergence test of Parseval's sum for $\partial G(x,\xi)/\partial n_x$ (imaginary part).

The convergence rate is examined by using the Parseval's sum in Figs.10(a) and 10(b), for real and imaginary parts, respectively. It is found that only few terms for Fourier series are required. In the real calculation, twenty terms are adopted. By changing the size of cylinder (a) and the same parameters of $\lambda = \pi$, $b = \frac{1}{2}\pi$, the relative amplitudes are shown in Figs.11 and 12 for different sizes of cylinders $a = 0.2\lambda$ and $a = 0.318\lambda$, respectively. Agreement with the Row's data is observed. By setting the fixed probe at ($2\lambda,0$),

the relative amplitudes versus the spacing between the two cylinders for $a = 0.2\lambda$, 0.24λ, 0.318λ, 0.477λ are shown in Figs.13-16, respectively, to see the effect of distance between the two cylinders for various sizes of cylinders. All the results in Figs.13-16 agree well with the theoretical and experimental data by Row [2].

Although only two cylinders are used in this proposed approach, our approach can be extended to deal with multiple cylinders problems. In this example, efficacy of the proposed method of the sound scattering problem is verified.
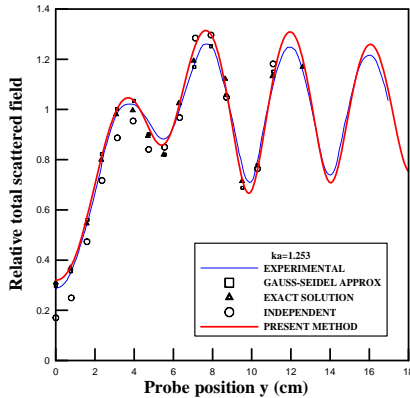
Fig. 11 Relative amplitude of total field versus the probe location (*M*=20).
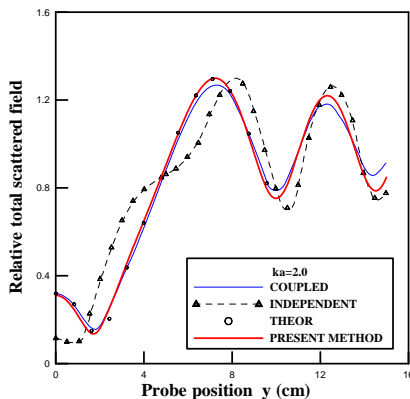
Fig. 12 Relative amplitude of total field versus the probe location (*M*=20).
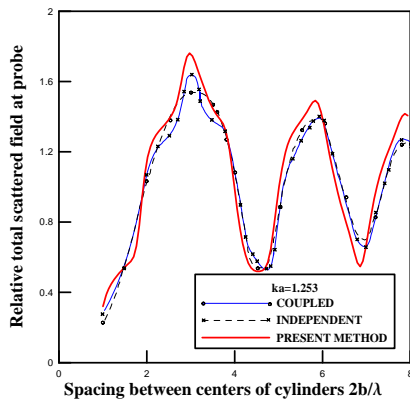
Fig. 13 Relative amplitude of total field versus $2b/\lambda$
($a = 0.2\lambda$ **and *M*=20).**
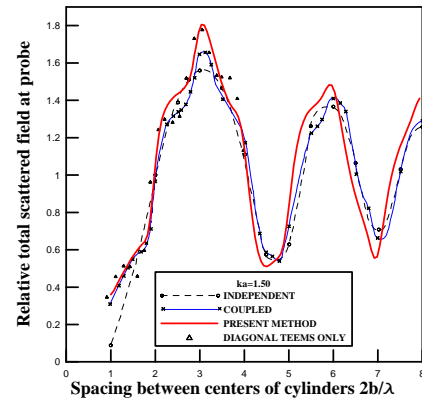
Fig. 14 Relative amplitude of total field versus $2b/\lambda$
($a = 0.24\lambda$ **and *M*=20).**
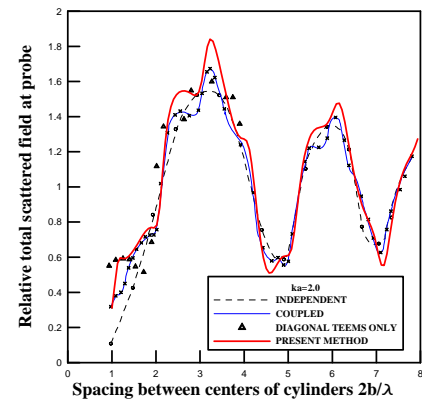
Fig. 15 Relative amplitude of total field versus $2b/\lambda$
($a = 0.318\lambda$ **and *M*=20).**
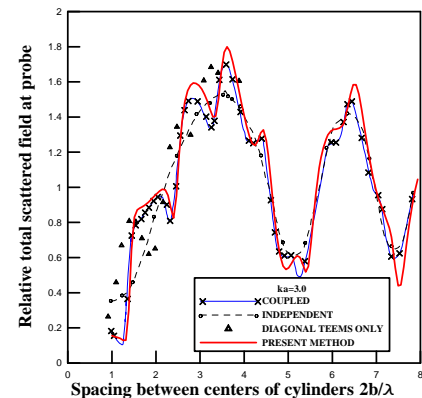
Fig. 16 Relative amplitude of total field versus $2b/\lambda$
($a = 0.477\lambda$ **and *M*=20)**.

In addition, it can be extended to deal with scattering problem in different engineering areas, *e.g.* water-wave problem or electromagnetism, by following the same concept.

5. CONCLUSIONS

In this paper, we proposed the addition theorem and superposition technique to solve the scattering problem of two identical cylinders subject to a point source. Regarding the BVP with circular boundaries, we have proposed a BIEM formulation by using degenerate

kernels, null-field integral equation and Fourier series in companion with adaptive observer system. This method is a semi-analytical approach for the problems with circular boundaries since only truncation error in the Fourier series is involved. The method shows great generality and versatility for the problems with multiple cylinders of arbitrary number, radii and positions. A general-purpose program for solving the problems with arbitrary number, size and various locations of circular cavities was developed. Therefore, not only the sound scattering problems from a point source but also electromagnetic scattering problems can be solved by using the present approach. Good agreement is observed after comparing with theoretical and experiment data.

6. REFERENCES

[1] P.A. Martin, *Multiple Scattering - Interaction of time-harmonic waves with N obstacles*, Cambridge University Press, New York; 2006.

[2] R.V. Row, "Theoretical and experimental study of electromagnetic scattering by two identical conducting cylinders," *J. Appl. Phys.*, vol. 26, pp. 666-675, 1955.

[3] R.V. Row, "Microwave diffraction measurements in a parallel-plate region," *J. Appl. Phys.*, vol. 24, pp. 1448-1452, 1953.

[4] S.E. Sherer, "Scattering of sound from axisymetric sources by multiple circular cylinders," *J. Acoust. Soc. Am.*, vol. 115, pp. 488-496, 2004.

[5] J.T. Chen, W.C. Shen and A.C. Wu, "Null-field integral equations for stress field around circular holes under anti-plane shear," *Engng. Anal. Bound. Elem.*, vol. 30, pp. 205-217, 2005.

[6] J.T. Chen, C.T. Chen and I.L. Chen, "Null-field integral equation approach for eigenproblems with circular boundaries," *J. Comput. Acoust.*, vol. 15, pp. 1-28, 2008.

[7] J.T. Chen, P.Y. Chen and C.T. Chen, "Surface motion of multiple alluvial valleys for incident plane SH-waves by using a semi-analytical approach," *Soil Dyn. Earthqu. Engng.*, vol.28, pp.58-72, 2008.

[8] J.T. Chen, C.T. Chen, P.Y. Chen and I.L. Chen, "A semi-analytical approach for radiation and scattering problems with circular boundaries," *Comput. Meth. Appl. Mech. Engng*, vol.196, pp. 2751–2764, 2008.

[9] J.T. Chen and J.N. Ke, "Derivation of anti-plane dynamic Green's function for several circular inclusions with imperfect interfaces," *Comp. Model. Engng. Sci.*, vol.29, pp.111-135, 2008.

[10] J.T. Chen, K.H. Chou and S.K. Kao, "Derivation of Green's function using addition theorem," *Mech. Res. Commun.*, Revised, 2008.

[11] K.H. Chou, *Applications of addition theorem and superposition technique to anti-plane problems with circular boundaries subject to concentrated force and screw dislocation*, Master Thesis, National Taiwan Ocean University, Keelung; 2008.

[12] J.T. Chen, W.C. Shen and A.C. Wu, "Null-field integral equations for stress field around circular holes under antiplane shear," *Engng. Anal. Bound. Elem.*, vol. 30, pp. 205-217, 2006.

[13] J.T. Chen, W.C. Shen and P.Y. Chen, "Analysis of circular torsion bar with circular holes using null-field approach," *Comp. Model. Engng. Sci.*, vol. 12, pp. 109-119 2006.

[14] J.T. Chen and A.C. Wu, "Null-field approach for piezoelectricity problems with arbitrary circular inclusions," *Engng. Anal. Bound. Elem.,* vol. 30, pp. 971-993, 2006.

[15] J.T. Chen and W.C. Shen, "Degenerate scale for multiply connected Laplace problems," *Mech. Res. Commun.,* vol. 34, pp. 69-77, 2007.

[16] J.T. Chen and A.C. Wu, "Null-field approach for the multi-inclusion problem under antiplane shears," *ASME J. Appl. Mech, vol. 74,* pp. 469-487, 2007.

[17] J.T. Chen and P.Y. Chen, "A semi-analytical approach for stress concentration of cantilever beams with holes under bending," *J. Mech.,* vol. 23, pp. 211-221, 2007.

[18] J.T. Chen, J.N. Ke and H.Z. Liao, "Construction of Green's function using null field integral approach for Laplace problems with circular boundaries," *Comp. Mater. and Conti.*, Accepted, 2008.

[19] J.T. Chen and W.C. Shen, "Null-field approach for Laplace problems with circular boundaries using degenerate kernels," *Numer. Methods Partial Differ. Equ.*, Accepted, 2008.

[20] J.T. Chen, C.C. Hsiao and S.Y. Leu, "Null-field approach for Laplace problems with circular boundaries using degenerate kernels," *ASME J. Appl. Mech.,* vol. 73, pp. 679-693, 2007.

[21] J.T. Chen, W.M. Lee and H.Z. Liao, Discussion: "Isotropic clamped-free thin annular circular plate subjected to a concentrated load (Ajayi O. Adewale, 2006, ASME J. Appl. Mech., 73, pp. 658-663)," *ASME J. Appl. Mech.*, Accepted, 2008.

[22] W.M. Lee, J.T. Chen and Y.T. Lee, "Free vibration analysis of circular plates with multiple circular holes using indirect BIEMs," *J. Sound Vib.*, vol. 304, pp. 811–830, 2007.

[23] W.M. Lee, J.T. Chen and Y.T. Lee, "Null-field integral equation approach for free vibration analysis of circular plates with multiple circular holes," *Comput. Mech.*, vol. 42, pp. 733–747, 2008.

[24] W.M. Lee, J.T. Chen and Y.T. Lee, "Analytical study and numerical experiments of true and spurious eigensolutions of free vibration of circular," *Engng. Anal. Bound. Elem.*, vol. 32, pp. 368–387, 2008.

[25] J.T. Chen, H.Z. Liao and W.M. Lee, "An analytical approach for the Green's functions of biharmonic problems with circular and annular domains," J. Mech., Accepted, 2008.